Inorg. Chem. **2004**, *43*, 2922–2931

Tetradentate Bis(*o*-iminobenzosemiquinonate(1–)) π Radical Ligands and Their *o*-Aminophenolate(1–) Derivatives in Complexes of Nickel(II), Palladium(II), and Copper(II)

Kil Sik Min, Thomas Weyhermüller, Eberhard Bothe, and Karl Wieghardt*

Max-Planck-Institut für Bioanorganische Chemie, Stiftstrasse 34-36, D-45470 Mülheim an der Ruhr, Germany

Received August 6, 2003

The coordination chemistries of the potential tetradentate ligands *N*,*N*′-bis(3,5-di-*tert*-butyl-2-hydroxyphenyl)-ethylenediamine, $H_4[L^1]$, the unsaturated analogue glyoxal-bis(2-hydroxy-3,5-di-*tert*-butylanil), $H_2[L^2]$, and *N*,*N*′-bis-(2-hydroxy-3,5-di-*tert*-butylphenyl)-2,2-dimethylpropylenediamine, $H_4[L^3]$, have been investigated with nickel(II), palladium(II), and copper(II). The complexes prepared and characterized are $[Ni^{II}(H_3L^1)_2]$ (**1**), $[Ni^{II}(HL^2)_2]\cdot{}^5/_8CH_2Cl_2$ (**2**), $[Ni^{II}(L^{3\bullet\bullet})]$ (**3**), $[Pd^{II}(L^{3\bullet\bullet})][Pd^{II}(H_2L^3)]$ (**4**), and $[Cu^{II}(H_2O)(L^4)]$ (**5**), where $(L^4)^{2-}$ is the oxidized diimine form of $(L^3)^{4-}$ and $(L^{3\bullet\bullet})^{2-}$ is the bis(*o*-iminosemiquinonate) diradical form of $(L^3)^{4-}$. The structures of compounds **1**–**5** have been determined by single crystal X-ray crystallography. In complexes **1** and **2**, the ligands $(H_3L^1)^-$ and $(HL^2)^-$ are tridentate and the nickel ions are in an octahedral ligand environment. The oxidation level of the ligands is that of an aromatic *o*-aminophenol. **1** and **2** are paramagnetic ($\mu_{eff} \sim 3.2\ \mu_B$ at 300 K), indicating an $S = 1$ ground state. The diamagnetic, square planar, four-coordinate complexes **3** and $[Pd^{II}(L^{3\bullet\bullet})]$ in **4** each contain two antiferromagnetically coupled *o*-iminobenzosemiquinonate(1–) π radicals. Diamagnetic $[Pd^{II}(H_2L^3)]$ in **4** forms an eclipsed dimer via four N–H···O hydrogen bonding contacts which yields a nonbonding Pd···Pd contact of 3.0846-(4) Å. Complex **5** contains a five-coordinate Cu^{II} ion and two *o*-aminophenolate(1–) halves in $(L^4)^{2-}$. The electrochemistries of complexes **3** and **4a** ($[Pd^{II}(L^{3\bullet\bullet})]$ of **4**) have been investigated, and the EPR spectra of the monocations and -anions are reported.

Introduction

In a series of papers,[1−9] we have recently unequivocally established that organic *o*-aminophenol molecules are redox-noninnocent *O*,*N*-coordinated ligands which can exist in different protonation and oxidation levels in coordination compounds, as shown schematically in Chart 1. These protonation and oxidation levels can be determined in a given compound by high quality single crystal X-ray crystallography because the C−C, C−N, and C−O distances vary in a systematic fashion upon stepwise one-electron oxidation of the ligands.

The synthesis of the tetradentate ligand *N*,*N*′-bis(3,5-di-*tert*-butyl-2-hydroxyphenyl)ethylenediamine, $H_4[L^1]$, and its unsaturated counterpart glyoxal-bis(2-hydroxy-3,5-di-*tert*-butylanil), $H_2[L^2]$, have been described in refs 10 and 11, respectively, but to the best of our knowledge their coordination chemistry has not been explored to date. These ligands are shown in Chart 2. In addition, we have synthesized for the first time the analogue *N*,*N*′-bis(2-hydroxy-3,5-di-*tert*-butylphenyl)-2,2-dimethylpropylenediamine, $H_4[L^3]$.

* Author to whom correspondence should be addressed. E-mail: wieghardt@mpi-muelheim.mpg.de.

(1) Verani, C. N.; Gallert, S.; Bill, E.; Weyhermüller, T.; Wieghardt, K.; Chaudhuri, P. *Chem. Commun.* **1999**, 1747.
(2) Chaudhuri, P.; Verani, C. N.; Bill, E.; Bothe, E.; Wehyermüller, T.; Wieghardt, K. *J. Am. Chem. Soc.* **2001**, *123*, 2213.
(3) Chun, H.; Verani, C. N.; Chaudhuri, P.; Bothe, E.; Bill, E.; Weyhermüller, T.; Wieghardt, K. *Inorg. Chem.* **2001**, *40*, 4157.
(4) Herebian, D.; Ghosh, P.; Chun, H.; Bothe, E.; Weyhermüller, T.; Wieghardt, K. *Eur. J. Inorg. Chem.* **2002**, 1957.
(5) Chun, H.; Chaudhuri, P.; Weyhermüller, T.; Wieghardt, K. *Inorg. Chem.* **2002**, *41*, 790.
(6) Chun, H.; Bill, E.; Bothe, E.; Weyhermüller, T.; Wieghardt, K. *Inorg. Chem.* **2002**, *41*, 5091.
(7) Sun, X.; Chun, H.; Hildenbrand, K.; Bothe, E.; Weyhermüller, T.; Neese, F.; Wieghardt, K. *Inorg. Chem.* **2002**, *41*, 4295.
(8) Chun, H.; Weyhermüller, T.; Bill, E.; Wieghardt, K. *Angew. Chem., Int. Ed.* **2001**, *40*, 2489.
(9) Min, K. S.; Weyhermüller, T.; Wieghardt, K. *J. Chem. Soc., Dalton Trans.* **2003**, 1126.
(10) Komissarov, V. N.; Ukhin, L. Yu.; Vetoshkina, L. V. *Zh. Org. Khim.* **1990**, *26*, 2188.
(11) Haeussler, H.; Jadamus, H. *Chem. Ber.* **1964**, *97*, 3051.

10.1021/ic0302480 CCC: $27.50
Published on Web 03/30/2004

Chart 1

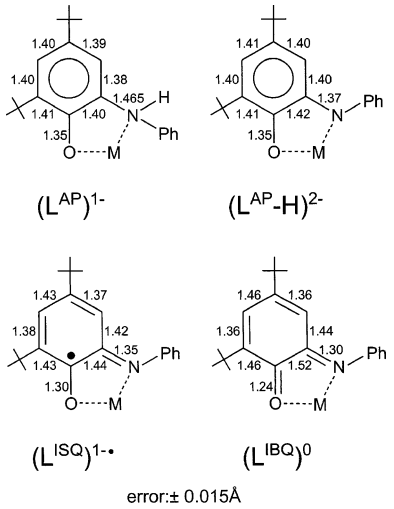

error:± 0.015Å

The coordination chemistries of these ligands with nickel(II), palladium(II), and copper(II) have been investigated in some detail here where we have placed special emphasis on *O*,*N*-coordinated *o*-iminobenzosemiquinonate π radical anions and a comparison of the geometrical details of bound saturated $(L^1)^{4-}$ versus unsaturated $(L^2)^{2-}$ ligands. The complexes prepared are listed in Chart 2.

Experimental Section

The ligands *N*,*N*′-bis(2-hydroxy-3,5-di-*tert*-butylphenyl)ethylenediamine, $H_4[L^1]$, and glyoxal-bis(2-hydroxy-3,5-di-*tert*-butylphenyl)imine, $H_2[L^2]$, have been prepared by slightly modified procedures described in refs 10 and 11.

***N*,*N*′-Bis(2-hydroxy-3,5-di-*tert*-butylphenyl)ethylenediamine, $H_4[L^1]$.** To a solution of 3,5-di-*tert*-butylcatechol (3.0 g; 13.5 mmol) in acetonitrile (30 mL) was added dropwise a solution of ethylenediamine (0.41 g; 6.75 mmol) in CH_3CN (2 mL) in the presence of air. After heating to reflux for 1 h, the solution was cooled to 20 °C and stirred for a further 3 h during which time a colorless precipitate of $H_4[L^1]$ formed which was collected by filtration, washed with *n*-hexane, and air-dried. Yield: 2.0 g (64%). ^{1}H NMR (500 MHz, DMSO-d_6, 300 K): δ 1.23 (s, 18H, CH_3 (*t*-Bu)), 1.35 (s, 18H, CH_3 (*t*-Bu)), 3.30 (s, 4H, CH_2), 4.70 (s, 2H, NH), 6.55 (d, 2H, CH (bz), J = 2.29 Hz), 6.56 (d, 2H, CH (bz), J = 2.29 Hz), 7.38 (s, 2H, OH). ^{13}C NMR (125 MHz, DMSO-d_6, 300 K): δ 29.9, 31.5 (CH_3 (*t*-Bu)), 34.0, 34.5 (*t*-Bu), 43.4 (ethylene), 107.0, 111.2, 136.1, 138.7, 140.4, 141.8 (C_{arom}). EI mass spectrometry: m/z = 468 (M^+). Anal. Calcd for $C_{30}H_{48}N_2O_2$: C, 76.87; H, 10.32; N, 5.98. Found: C, 76.59; H, 10.31; N, 5.75.

Glyoxal-bis(2-hydroxy-3,5-di-*tert*-butylphenyl)imine, $H_2[L^2]$. To a solution of 3,5-di-*tert*-butylbenzoquinone (3.0 g; 13.6 mmol) in MeCN (30 mL) was added dropwise a solution of ethylenediamine (0.41 g; 6.80 mmol) in CH_3CN (2 mL) at 0 °C in the presence of air. The resulting mixture was stirred at 0 °C for 1 h after which time a yellow (brownish) precipitate was collected by filtration, washed with petroleum ether, and air-dried. Yield: 1.6 g (51%). ^{1}H NMR (400 MHz, CD_2Cl_2, 300 K): δ 1.35 (s, 18H, CH_3 (*t*-Bu)), 1.45 (s, 18H, CH_3 (*t*-Bu)), 7.31 (d, 2H, CH (bz)), J = 2.22 Hz), 7.36 (d, 2H, CH (bz), J = 2.20 Hz), 7.89 (s, 2H, OH), 8.65 (s, 2H, NCH). ^{13}C NMR (100 MHz, CD_2Cl_2, 300 K): δ 29.5, 31.7 (CH_3 (*t*-Bu)), 34.9, 35.3 (*t*-Bu), 110.4, 126.3, 134.0, 136.2, 142.2, 150.37 (C_{arom}), 155.1 (ethylene). EI mass spectrometry: m/z = 464 (M^+). Anal. Calcd for $C_{30}H_{44}N_2O_2$: C, 77.54; H, 9.54; N, 6.03. Found: C, 77.38; H, 9.38; N, 6.14.

Chart 2

Ligands

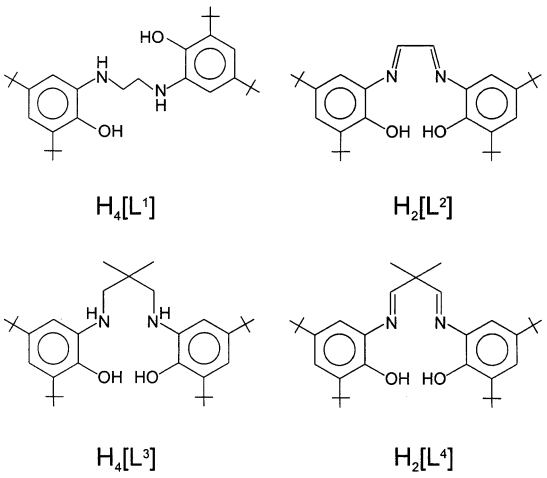

Complexes

$[Ni^{II}(H_3L^1)_2]$	(**1**)
$[Ni^{II}(HL^2)_2] \cdot 0.6\ CH_2Cl_2$	(**2**)
$[Ni^{II}(L^{3\bullet\bullet})]$	(**3**)
$[Pd^{II}(L^{3\bullet\bullet})]\ [Pd^{II}(H_2L^3)]$	(**4**)
$[Cu^{II}(H_2O)(L^4)]$	(**5**)

***N*,*N*′-Bis(2-hydroxy-3,5-di-*tert*-butylphenyl)-2,2-dimethylpropylenediamine, $H_4[L^3]$.** To a solution of 3,5-di-*tert*-butylcatechol (3.0 g; 13.5 mmol) in CH_3CN (30 mL) was added dropwise a solution of 2,2-dimethylpropylenediamine (0.69 g; 6.75 mmol) in MeCN (2 mL) in the presence of air. After heating to reflux for 30 min, the solution was cooled to room temperature. A colorless precipitate was isolated by filtration and washed with *n*-hexane. Yield: 2.1 g (62%). ^{1}H NMR (400 MHz, CD_2Cl_2, 300 K): δ 1.13 (s, 6H, CH_3 (methyl)), 1.29 (s, 18H, CH_3 (*t*-Bu)), 1.39 (s, 18H, CH_3 (*t*-Bu)), 2.96 (s, 4H, CH_2), 6.88 (arom H, 2H), 6.98 (arom H, 2H). EI mass spectrometry: m/z = 510 (M^+). Anal. Calcd for $C_{33}H_{54}N_2O_2$: C, 77.60; H, 10.66; N, 5.48. Found: C, 77.54; H, 10.62; N, 5.56.

$[Ni(H_3L^1)_2]$ (1). To a solution of the ligand $H_4[L^1]$ (468 mg; 1.0 mmol) in EtOH (30 mL) was added dropwise with stirring a solution of $Ni(NO_3)_2 \cdot 6H_2O$ (146 mg; 0.5 mmol) in EtOH (5 mL) at room temperature in the presence of air. From this solution, a microcrystalline pink precipitate formed within 1 h which was collected by filtration, washed with EtOH, and air-dried. Single crystals of **1**·4MeOH suitable for X-ray crystallography were obtained by solvent diffusion of MeOH into a CH_3Cl solution of **1**. Yield: 470 mg (95%). EI mass spectrometry: m/z = 992 (M^+). Anal. Calcd for $C_{60}H_{94}N_4NiO_4$: C, 72.49; H, 9.53; N, 5.64. Found: C, 72.36; H, 9.68; N, 5.66.

$[Ni(HL^2)_2] \cdot {}^5/_8CH_2Cl_2$ (2·$^5/_8CH_2Cl_2$). A solution of triethylamine (0.14 mL; 1.0 mmol) in CH_3CN (5 mL) was added to a slurry of $Ni^{II}(NO_3)_2 \cdot 6H_2O$ (73 mg; 0.25 mmol) and the ligand $H_2[L^2]$ (234 mg; 0.5 mmol) in CH_3CN (20 mL) in the presence of air, causing immediate dissolution of the ligand and formation of a dark green solution. The mixture was stirred for 3 h during which time a deep green precipitate formed. The crude product was recrystallized from CH_2Cl_2 to afford deep green microcrystals of **2**·$^5/_8CH_2Cl_2$. Single crystals suitable for X-ray crystallography were obtained by solvent diffusion of MeOH into a CH_2Cl_2 solution of **2**. Yield: 190 mg (74%). ESI mass spectrometry in CH_2Cl_2 (positive ion mode): m/z = 985 $(M + H)^+$. Anal. Calcd for $C_{60}H_{86}N_4NiO_4$ ($^5/_8CH_2Cl_2$): C, 70.07; H, 8.46; N, 5.39. Found: C, 69.98; H, 8.40; N, 5.28.

[Ni($L^{3\bullet}$)] (3). To a solution of $Ni^{II}(NO_3)_2 \cdot 6H_2O$ (0.29 g; 1.0 mmol) in CH_3CN (40 mL) was added with stirring solid $H_4[L^3]$ (0.51 g; 1.0 mmol) and triethylamine (0.56 mL; 4.0 mmol) at room temperature in the presence of air. From this solution, a microcrystalline dark green precipitate formed within 1 h which was collected by filtration, washed with cold CH_3OH, and air-dried. Single crystals of **3** suitable for X-ray crystallography were obtained by solvent diffusion of CH_3OH into a CH_2Cl_2 solution of **3**. Yield: 0.32 g (57%). ^1H NMR (400 MHz, CD_2Cl_2, 300 K): δ 1.27 (s, 18H, CH_3 (*t*-Bu)), 1.43 (s, 6H, CH_3 (methyl)), 1.50 (s, 18H, CH_3 (*t*-Bu)), 3.47 (s, 4H, CH_2), 6.83 (arom H, 2H), 7.10 (arom H, 2H). EI mass spectrometry: $m/z = 564$ (M^+). Anal. Calcd for $C_{33}H_{50}N_2NiO_2$: C, 70.10; H, 8.91; N, 4.95. Found: C, 69.85; H, 8.82; N, 5.06.

[Pd($L^{3\bullet}$)][Pd(H_2L^3)] (4). To a solution of $Pd^{II}(CH_3CO_2)_2$ (0.11 g; 0.5 mmol) in CH_3OH (15 mL) was added with stirring solid $H_4[L^3]$ (0.26 g; 0.5 mmol) and triethylamine (0.28 mL; 2.0 mmol) at room temperature in the presence of air. From this solution, a microcrystalline dark green precipitate formed within 3 h which was collected by filtration, washed with cold CH_3OH, and air-dried. Single crystals of **4** suitable for X-ray crystallography were obtained by solvent diffusion of CH_3OH into a CH_2Cl_2 solution of **4**. Yield: 0.15 g (49%). We then separated **4** into dark green [$Pd^{II}(L^{3\bullet})$] (**4a**) and yellow $[Pd^{II}(H_2L^3)]_2$ (**4b**) by high-pressure liquid chromatography on a Nucleosil-7-C18 column (Gilson m305 pump, UV−vis detector operating at 300 nm) at a 6 mL/min flow rate with 2% CH_2Cl_2/MeCN as eluent. [Pd($L^{3\bullet}$)] (**4a**) ^1H NMR (400 MHz, CD_2Cl_2, 300 K): δ 1.10 (s, 18H, CH_3 (*t*-Bu)), 1.28 (s, 18H, CH_3 (*t*-Bu)), 1.41 (s, 6H, CH_3 (methyl)), 2.84 (m, 4H, CH_2), 6.63 (arom H, 2H), 6.71 (arom H, 2H). EI mass spectrometry: $m/z = 612$ (M^+). Anal. Calcd for $C_{33}H_{50}N_2PdO_2$: C, 64.64; H, 8.22; N, 4.57. Found: C, 64.65; H, 8.10; N, 4.41. [Pd(H_2L^3)] (**4b**) ^1H NMR (400 MHz, CD_2Cl_2, 300 K): δ 1.32 (s, 18H, CH_3 (*t*-Bu)), 1.46 (s, 18H, CH_3 (*t*-Bu)), 1.54 (s, 6H, CH_3 (methyl)), 1.58 (s, 4H, CH_2), 7.22 (arom H, 2H), 7.54 (s, 2H, NH). EI mass spectrometry: $m/z = 1230$ (M^+). Anal. Calcd for $C_{33}H_{52}N_2PdO_2$: C, 64.43; H, 8.52; N, 4.55. Found: C, 64.34; H, 8.60; N, 4.62.

[Cu(H_2O)(L^4)] (5). To a solution of $Cu^{II}Cl_2 \cdot 2H_2O$ (85 mg; 0.5 mmol) in CH_3OH (20 mL) was added with stirring solid H_4L^3 (0.26 g; 0.5 mmol) and triethylamine (0.28 mL; 2.0 mmol) at room temperature. The mixture was stirred for 30 min in the presence of air. The dark green solution was allowed to stand under an argon blanketing atmosphere until dark brown crystals formed which were collected by filtration, washed with CH_3OH, and air-dried. Yield: 0.13 g (45%). EI mass spectrometry: $m/z = 567$ ($M - H_2O$)$^+$. Anal. Calcd for $C_{33}H_{50}N_2CuO_3$: C, 67.60; H, 8.59; N, 4.78. Found: C, 67.91; H, 8.41; N, 4.72.

2,2-Bis(5,7-di-*tert*-butyl-benzoxazol-2-yl)-propane (6). To a solution of $Pd^{II}Cl_2$ (89 mg; 0.5 mmol) in CH_3OH (20 mL) was added with stirring solid H_4L^3 (0.26 g; 0.5 mmol) and triethylamine (0.28 mL; 2.0 mmol) at room temperature. After being stirred for 30 min in the presence of air, the brown solution was filtered. The resulting solution was allowed to stand under an argon blanketing atmosphere until colorless crystals formed which were collected by filtration, washed with CH_3OH, and air-dried. Yield: 0.13 g (50%). ^1H NMR (400 MHz, CD_2Cl_2, 300 K): δ 1.36 (s, 18H, CH_3 (*t*-Bu)), 1.42 (s, 18H, CH_3 (*t*-Bu)), 2.03 (s, 6H, CH_3 (methyl)), 7.28 (arom H, 2H), 7.55 (arom H, 2H). EI mass spectrometry: $m/z = 502$ (M^+). Anal. Calcd for $C_{33}H_{46}N_2O_2$: C, 78.84; H, 9.22; N, 5.57. Found: C, 78.65; H, 9.15; N, 5.45.

Physical Measurements. Electronic spectra of the complexes and spectra of the spectroelectrochemical investigations were recorded on an HP 8452A diode array spectrophotometer in the range 190−1100 nm. Cyclic voltammograms, square-wave voltammograms, and coulometric experiments were performed using an EG&G potentiostat/galvanostat. EI and ESI mass spectra were recorded on a Finnigan MAT 8200, a Finnigan MAT 95, or a HP 5989 mass spectrometer. ^1H NMR spectra were measured on Bruker DRX 400 or DRX 500 spectrometers using the solvent as internal standard. Temperature-dependent (2−298 K) magnetization data were recorded on a SQUID magnetometer (MPMS Quantum Design) in an external magnetic field of 1.0 T. The experimental susceptibility data were corrected for underlying diamagnetism by the use of tabulated Pascal's constants. X-band EPR spectra were recorded on a Bruker ESP ELEXSYS E500 spectrometer equipped with a helium flow cryostat (Oxford Instruments ESR 910). The spectra were simulated by iteration of the anisotropic *g* values, hyperfine coupling constants, and line widths.

X-ray Crystallographic Data Collection and Refinement of the Structures. Dark green single crystals of **2**, **3**, **4**, and **6** (light green), yellow-brown crystals of **5**, and pale pink crystals of **1** were coated with perfluoropolyether, were picked up with a glass fiber, and were immediately mounted in the nitrogen cold stream to prevent loss of solvent. Intensity data were collected at 100 K using a Nonius Kappa-CCD diffractometer equipped with a Mo-target rotating-anode X-ray source and a graphite monochromator (Mo Kα, $\lambda = 0.71073$ Å). Final cell constants were obtained from a least-squares fit of a subset of several thousand strong reflections. Data collection was performed by hemisphere runs taking frames at 1.0° (**1**, **3**, **4**, and **6**), 0.7° (**2**), and 0.5° (**5**) in angular frequency (ω). Crystal faces of **2**, **4**, and **6** were determined, and the corresponding intensity data were corrected for absorption using the Gaussian-type routine embedded in XPREP.[13] Data sets of the other compounds were left uncorrected. Crystallographic data of the compounds are listed in Table 1. The Siemens ShelXTL[13] software package was used for the solution and the artwork of the structure and ShelXL97[14] was used for the refinement. The structures were readily solved by direct and Patterson methods and subsequent difference Fourier techniques. All non-hydrogen atoms were refined anisotropically, and hydrogen atoms were placed at calculated positions and refined as riding atoms with isotropic displacement parameters.

Results and Discussion

Syntheses and Characterization. The reaction of an ethanolic solution of the ligand *N*,*N*′-bis(2-hydroxy-3,5-di-*tert*-butylphenyl)ethylenediamine, $H_4[L^1]$, with $Ni(NO_3)_2 \cdot 6H_2O$ (ratio 2:1) in ethanol at 20 °C resulted in the formation of a pink precipitate of $[Ni^{II}(H_3L^1)_2]$ (**1**). From a similar reaction of the unsaturated analogue glyoxal-bis(2-hydroxy-3,5-di-*tert*-butylphenyl)imine, $H_2[L^2]$, in acetonitrile with triethylamine and $Ni^{II}(NO_3)_2 \cdot 6H_2O$, a dark green precipitate of $[Ni^{II}(HL^2)_2]$ was obtained which was recrystallized from CH_2Cl_2 as $[Ni^{II}(HL^2)_2] \cdot {}^5/_8CH_2Cl_2$ (**2**$\cdot {}^5/_8CH_2Cl_2$).

In contrast, when $Ni^{II}(NO_3)_2 \cdot 6H_2O$ reacted with the new ligand *N*,*N*′-bis(2-hydroxy-3,5-di-*tert*-butylphenyl)-2,2-dimethylpropylenediamine, $H_4[L^3]$ (1:1), in the presence of air in acetonitrile and NEt_3 at ambient temperature, a dark green precipitate of [$Ni^{II}(L^{3\bullet})$] (**3**) formed in 57% yield. Here, $(L^{3\bullet})^{2-}$ represents the two electron oxidized bis(π radical

(12) Ghosh, P.; Bill, E.; Weyhermüller, T.; Neese, F.; Wieghardt, K. *J. Am. Chem. Soc.* **2003**, *125*, 1293.
(13) *ShelXTL*, version 5; Siemens Analytical X-ray Instruments, Inc.: 1994.
(14) Sheldrick, G. M. *ShelXTL97*; Universität Göttingen: Germany, 1997.

Table 1. Crystallographic Data of Complexes

	1·4MeOH	**2**·$^5/_8CH_2Cl_2$	**3**	**4**	**5**	**6**
chem formula	$C_{64}H_{110}N_4NiO_8$	$C_{60.63}H_{87.3}N_4NiO_4Cl_{1.3}$	$C_{33}H_{50}N_2NiO_2$	$C_{66}H_{102}N_4O_4Pd_2$	$C_{33}H_{50}CuN_2O_3$	$C_{33}H_{46}N_2O_2$
fw	1122.27	1039.12	565.46	1228.32	586.29	502.72
space group	$P\bar{1}$, No. 2	$P2_1/c$, No. 14	$P\bar{1}$, No. 2	$P\bar{1}$, No. 2	$P2_1/m$, No. 11	$P2_1/c$, No. 14
a, Å	9.3467(6)	27.8848(8)	10.3164(3)	10.2622(4)	5.8251(9)	10.5174(3)
b, Å	12.7603(9)	17.7912(6)	10.4724(3)	17.3141(6)	33.067(5)	20.0475(6)
c, Å	15.6090(9)	26.7871(8)	16.1228(6)	19.0743(8)	8.086(2)	29.0130(9)
α, deg	112.89(1)	90	103.22(1)	97.118(1)	90	90
β, deg	95.38(1)	115.52(1)	98.95(1)	98.00(1)	92.54(3)	96.79(1)
γ, deg	104.83(1)	90	106.08(1)	107.13(1)	90	90
V, Å	1618.4(2)	11992.6(6)	1584.11(9)	3158.3(2)	1556.0(5)	6074.4(3)
Z	1	8	2	2	2	8
T, K	100(2)	100(2)	100(2)	100(2)	100(2)	100
ρ calcd, g cm^{-3}	1.152	1.151	1.185	1.292	1.251	1.099
reflns collected/2Θ$_{max}$	20075/66.30	103713/59.16	45276/66.00	108652/62.00	9855/42.00	111282/52.82
unique reflns/$I > 2\sigma(I)$	12291/8684	33485/26299	11858/8481	20077/15177	1676/1102	12422/9463
no. of params/restraints	372/0	1349/7	357/0	719/0	184/0	722/132
μ(Mo Kα), cm^{-1}	3.53	4.25	6.42	6.17	7.36	0.67
R1[a]/ goodness of fit[b]	0.0578/1.018	0.0682/1.133	0.0534/1.018	0.0397/1.030	0.0951/1.068	0.0583/1.047
wR2[c] ($I > 2\sigma(I)$)	0.1214	0.1425	0.1156	0.0774	0.1714	0.1182

[a] Observation criterion: $I > 2\sigma(I)$. $R1 = \sum||F_o| - |F_c||/\sum|F_o|$. [b] $GOF = [\sum[w(F_o^2 - F_c^2)^2]/(n-p)]^{1/2}$. [c] $wR2 = [\sum[w(F_o^2 - F_c^2)^2]/\sum[w(F_o^2)^2]]^{1/2}$, where $w = 1/\sigma^2(F_o^2) + (aP)^2 + bP$ and $P = (F_o^2 + 2F_c^2)/3$.

anion) of the deprotonated ligand $(L^3)^{4-}$; the ligand contains two *O*,*N*-coordinated *o*-iminobenzosemiquinonate(1−) radicals.

In a similar reaction of $H_4[L^3]$ and $Pd^{II}(CH_3CO_2)_2$ (1:1) in methanol in the presence of air and NEt_3, a dark green precipitate of cocrystallizing $[Pd^{II}(L^{3\bullet\bullet})][Pd^{II}(H_2L^3)]$ (**4**) was obtained. It is possible to separate the two neutral complexes from a CH_2Cl_2/CH_3CN solution of **4**. Two distinct compounds, namely, dark green $[Pd^{II}(L^{3\bullet\bullet})]$ (**4a**) and yellow $[Pd^{II}(H_2L^3)]_2$ (**4b**), were obtained from high-pressure liquid chromatography. Both complexes are diamagnetic, as was judged from their normal (but differing!) ^1H NMR spectra (see the Experimental Section). It is interesting to note that the dimeric nature of the $[Pd^{II}(H_2L^3)]_2$ complex remains intact in solution. The EI mass spectrum displays a molecular ion peak (M_2^+) at $m/z = 1230$, whereas the corresponding $[Pd^{II}(L^{3\bullet\bullet})]$ complex is mononuclear ($m/z = 612$ (M^+)).

In an attempt to generate the corresponding $[Cu^{II}(L^{3\bullet\bullet})]$ complex, a methanolic solution of $Cu^{II}Cl_2 \cdot 2H_2O$ was treated with an equivalent of $H_4[L^3]$ and NEt_3 in the presence of air at ambient temperature. Dark brown crystals of $[Cu^{II}(H_2O)(L^4)]$ (**5**) were obtained in 45% yield. $(L^4)^{2-}$ is the oxidized diimine form of $H_4(L^3)$, as shown in Chart 2. Thus, the desired product $[Cu^{II}(L^{3\bullet\bullet})]$ has not been obtained.

When $Pd^{II}Cl_2$ was used as starting material instead of $Pd^{II}(CH_3CO_2)_2$ in the above reaction yielding **4** under otherwise identical reaction conditions, colorless crystals of 2,2-bis(5,7-di-*tert*-butylbenzooxazol-2-yl)propane (**6**) were obtained in 50% yield, according to Scheme 1.

From temperature-dependent magnetic susceptibility measurements at 1.0 T in the range 2−300 K, it was established that complexes **1** and **2** are paramagnetic. Temperature-independent (20−290 K) magnetic moments of 3.1 μ_B for **1** with $g = 2.12$ and 3.2 μ_B for **2** with $g = 2.13$ indicate an $S = 1$ ground state for both complexes. Zero-field splitting parameters of 4 cm^{-1} for **1** and 6 cm^{-1} for **2** were calculated from a fitting to the low temperature (<20 K) data. These values are typical for octahedral Ni^{II} complexes. In contrast,

Scheme 1

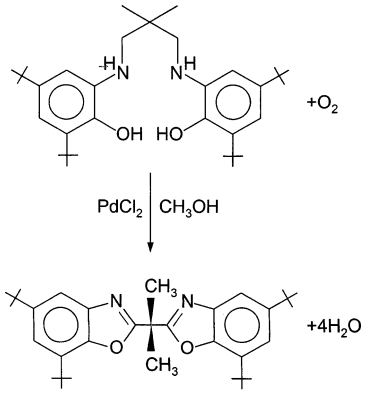

6

Table 2. Electronic Spectra of Complexes at 22 °C in CH_2Cl_2 Solution

complex	λ_{max}, nm (ϵ, L mol^{-1} cm^{-1})
1	551 (12), 886 (12)
2	388 (2.6×10^4), 623 (1.7×10^4)
3	293 (1.4×10^4), 416 (1.6×10^3), 581 (1.7×10^3), 854 (3.0×10^4)
$[Pd(L^{3\bullet\bullet})]$ **(4a)**	302 (1.9×10^4), 434 (3.1×10^4), 522 (2.4×10^3, sh), 559 (2.9×10^3), 843 (3.1×10^4)
$[Pd(H_2L^3)]$ **(4b)**	294 (1.9×10^4), 419 (8.6×10^3)
5	409 (9.6×10^3), 560 (460)

complex **3** is diamagnetic ($S = 0$), as is expected for a square planar Ni^{II} ion coordinated to two ligand π radicals.[2,15−18]

The electronic spectra of complexes **1** and **2** are summarized in Table 2 and shown in Figure 1. The spectrum of **1** displays two spin allowed d−d transitions of low intensities ($\epsilon < 20$ M^{-1} cm^{-1}) in the visible spectrum, which is characteristic for an octahedral Ni^{II} (d^8) ion, whereas the spectrum of **2** appears to be dominated by an intense ($\epsilon > 10^4$ M^{-1} cm^{-1}) metal-to-ligand or ligand-to-ligand (Scheme

(15) Balch, A. L.; Holm, R. H. *J. Am. Chem. Soc.* **1966**, *88*, 5201.
(16) Holm, R. H.; Balch, A. L.; Davison, A.; Maki, A.; Berry, T. *J. Am. Chem. Soc.* **1967**, *89*, 2866.
(17) Forbes, C. E.; Gold, A.; Holm, R. H. *Inorg. Chem.* **1971**, *10*, 2479.
(18) Stiefel, E. I.; Waters, J. H.; Billig, E.; Gray, H. B. *J. Am. Chem. Soc.* **1965**, *87*, 3016.

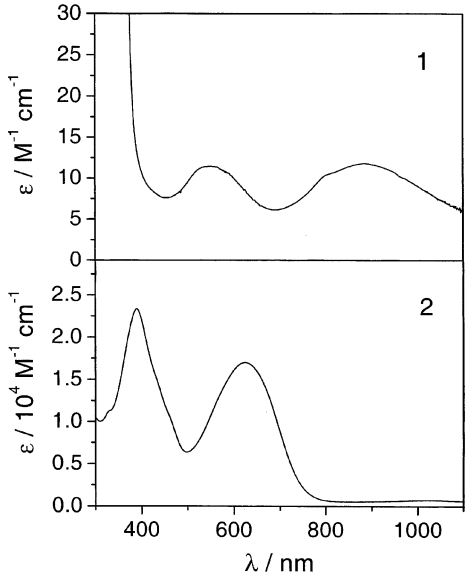

Figure 1. Electronic spectra of **1** in CH_2Cl_2 containing 1 mM $[BH_4]^-$ as reductant (top) and of **2** in CH_2Cl_2 at 20 °C (bottom). Note the difference of scales of the molar extinction coefficients of **1** and **2**.

Scheme 2

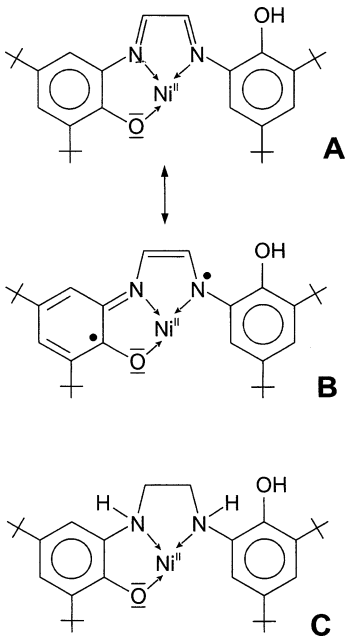

2) charge transfer band in the visible spectrum. The spectra of **3** and $[Pd^{II}(L^{3\bullet\bullet})]$ (**4a**) are very similar to those reported for other square planar $[M^{II}(L^{ISQ})_2]$ (M^{II} = Ni, Pd) complexes, where $(L^{ISQ})^{-\bullet}$ is an *o*-iminobenzosemiquinonate(1−) π radical anion.[2] The most characteristic feature of these bis(radical) species is the very intense (>10^4 L mol^{-1} cm^{-1}) ligand-to-ligand charge transfer band at 854 nm for **3** and at 843 nm for **4a**.

Electro- and Spectroelectrochemistry. Cyclic voltammograms (CVs) of **3** and **4a** have been recorded in CH_2Cl_2 solutions containing 0.10 M $[N(n\text{-}Bu)_4]PF_6$ as supporting electrolyte by a glassy carbon working electrode and a Ag/$AgNO_3$ reference electrode. Ferrocene was used as internal standard, and all potentials are referenced versus the ferrocenium/ferrocene couple (Fc^+/Fc).

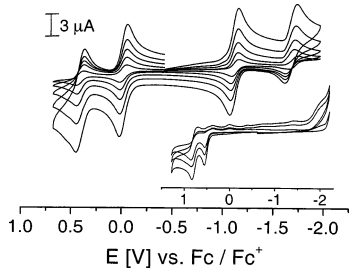

Figure 2. Cyclic voltammograms of **4a** in CH_2Cl_2 solution (0.10 M $[N(n\text{-}Bu)_4]PF_6$) at 20 °C recorded by a glassy carbon working electrode at scan rates of 50, 100, 200, 400, and 800 mV s^{-1}. The inset shows the CVs of **4b** in CH_2Cl_2 at scan rates of 100, 200, and 400 mV s^{-1}.

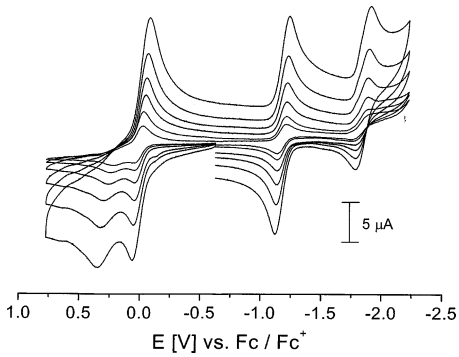

Figure 3. Cyclic voltammograms of **3** in CH_2Cl_2 solution (0.10 M $[N(n\text{-}Bu)_4]PF_6$) at 20 °C recorded by a glassy carbon working electrode at scan rates of 25, 50, 100, 200, 400, and 800 mV s^{-1}.

Figure 2 shows the CV of **4a** and as the inset that of the dimer **4b**. The CV of **4a** displays four reversible one-electron transfer waves ($E^1_{1/2} = 0.40$, $E^2_{1/2} = -0.03$, $E^3_{1/2} = -1.13$, and $E^4_{1/2} = -1.68$ V). Coulometric experiments at appropriately fixed potentials establish that the first two correspond to two successive one-electron oxidations of **4a**, whereas the latter two are successive one-electron reductions. The CV of **4b** displays two irreversible oxidations at peak potentials of 0.85 and 0.54 V, which have not been investigated in further detail. These data correspond exactly to those reported[2] for *trans*-$[Pd^{II}(L^{ISQ})_2]$: $E^{1-4}{}_{1/2} = 0.47$, 0.08, −0.99, and −1.40. It was shown that these processes are ligand centered rather than metal centered, as shown in eq 1, where (L^{IBQ}) represents the neutral *o*-iminobenzoquinone, $(L^{ISQ})^{-\bullet}$ represents the *o*-iminobenzosemiquinonate π radical, and $(L^{AP}-H)^{2-}$ is the *o*-iminophenolate dianion.

$$[M^{II}(L^{IBQ})_2]^{2+} \underset{+e}{\overset{-e}{\rightleftharpoons}} [M^{II}(L^{IBQ})(L^{ISQ})]^{+} \underset{+e}{\overset{-e}{\rightleftharpoons}} [M^{II}(L^{ISQ})_2] \underset{+e}{\overset{-e}{\rightleftharpoons}} [M(L^{AP}-H)(L^{ISQ})]^{-} \underset{+e}{\overset{-e}{\rightleftharpoons}} [M^{II}(L^{AP}-H)_2]^{2-} \quad (1)$$

Figure 3 exhibits the corresponding CV of nickel analogue **3** where also four one-electron transfer waves are observed at 0.26, −0.00, −1.18, and −1.84 V. The latter three waves are clearly reversible, whereas in the process $E^1_{1/2}$ is not well separated from $E^2_{1/2}$ and the value 0.26 V corresponds to a peak potential. Again, the CV of *trans*-$[Ni^{II}(L^{ISQ})_2]$ is very similar: at 0.042 V, a reversible two-electron transfer oxidation has been observed, but at −1.07 and −1.64 V, two reversible one-electron reductions have been reported. Such complete (or incomplete) electron transfer series have

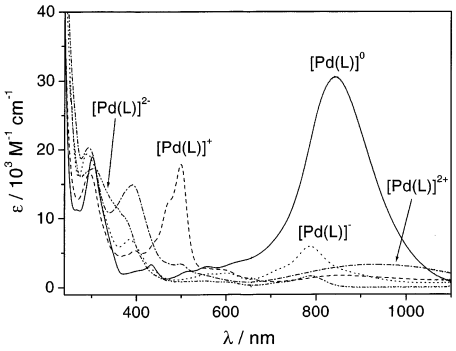

Figure 4. Electronic spectra of **4a** and its electrochemically generated mono- and dications and mono- and dianions in CH_2Cl_2 solution (0.10 M $[N(n\text{-}Bu)_4]PF_6$).

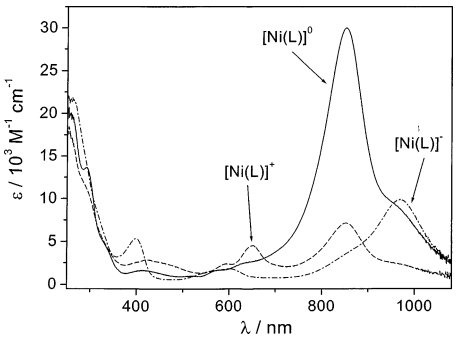

Figure 5. Electronic spectra of neutral **3** and its electrochemically generated monoanion and monocation (0.10 M $[N(n\text{-}Bu)_4]PF_6$).

been reported for many square planar Ni^{II}, Pd^{II}, and Pt^{II} complexes containing two catecholate, phenylenediamide, benzodithiolate, or *o*-iminothiophenolate ligands.[15−18]

Controlled-potential coulometry allows the selective generation of the stable mono- and dications as well as the mono- and dianions of **4a** of which the respective electronic spectra have been recorded. These are shown in Figure 4. Similarly, the spectra of neutral **3**, its monocation, and its monoanion are shown in Figure 5. These spectra are again very similar to those reported for the oxidized and reduced forms of $[M^{II}(L^{ISQ})_2]$ (M = Ni or Pd).[2]

It is interesting that both the monocations and the monoanions are paramagnetic ($S = {}^1/_2$) mixed valent compounds which belong to class III according to Robin and Day[19] where the unpaired electron is delocalized over both ligands (or both halves of the ligand in **3** and **4a**). This has been explicitly shown by DFT calculations and spectroscopy for the monocations and -anions of bis(3,5-di-*tert*-butyl-*o*-diiminobenzosemiquinonate)nickel(II) and $[Pt^{II}(L^{ISQ})_2]$ in refs 20 and 7, respectively.

Crystal Structures. Single crystal X-ray structure determinations of complexes **1**, **2**, **3**, **4**, **5**, and **6** have been carried out at 100 K. Table 1 summarizes crystallographic data, and Table 3 lists selected bond distances of the compounds.

Crystals of **1** consist of well-separated neutral molecules of $[Ni^{II}(H_3L^1)_2]$ where an octahedral Ni^{II} ion is facially coordinated to two tridentate monoanions $(H_3L^1)^-$. The molecule possesses crystallographic C_i symmetry. Figure 6 shows such a molecule. Each ligand consists of an *O*,*N*-coordinated *o*-aminophenolate(1−) half and a dangling *o*-aminophenol part, both of which are *N*,*N*-connected by an ethyl bridge, and the latter forms an intramolecular O−H···O bond (O1···O16, 2.538(3) Å). It is an important feature of this structure that the 12 C−C bonds in both phenyl rings of the $(H_3L^1)^-$ ligand are nearly equidistant (av 1.399 Å) and typical for an aromatic six-membered ring. The C−O and C−N bond lengths of the coordinated and dangling part of the ligand also indicate the $(L^{AP})^-$ character (Chart 1) of these ligands.

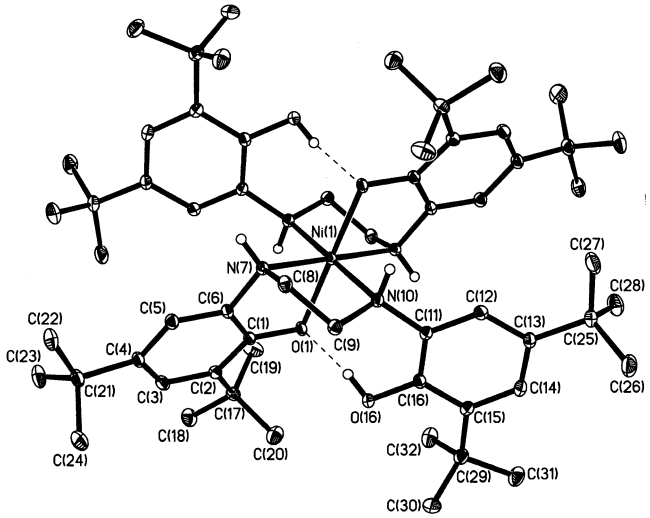

Figure 6. Structure of a neutral molecule $[Ni^{II}(H_3L^1)_2]$ in crystals of **1**. Intramolecular hydrogen bonding: O1···O16, 2.538(3) Å.

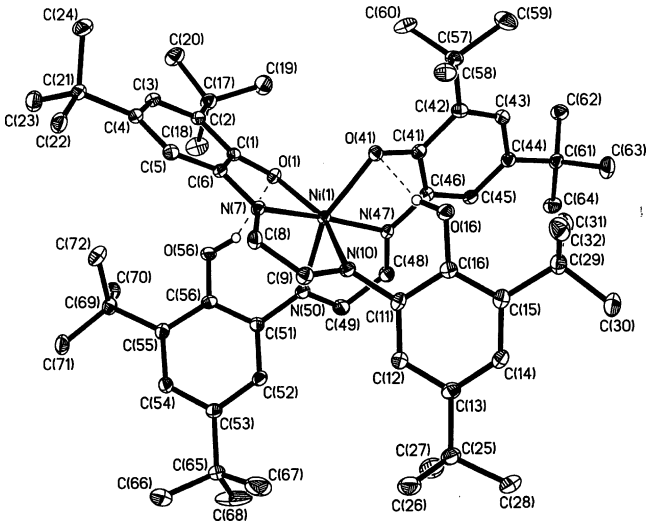

Figure 7. Structure of a neutral molecule $[Ni^{II}(HL^2)_2]$ in crystals of **2**. Intramolecular hydrogen bonding: O1···O56, 2.697(4) Å; O16···O41, 2.764(4) Å.

Figure 7 displays the structure of the neutral molecule $[Ni^{II}(HL^2)_2]$ in crystals of **2**. There are two crystallographically independent molecules with nearly identical structures. Superficially, their structures are very similar to that of **1**, but clearly, the two *o*-aminophenol(ate) halves are covalently *N*,*N*′-bound to an unsaturated ethylene bridge and both nitrogen atoms of the $(HL^2)^-$ ligand are sp^2 hybridized.

(19) Robin, M. B.; Day, P. *Adv. Inorg. Chem. Radiochem.* **1967**, *10*, 247.
(20) Bachler, V.; Olbrich, G.; Neese, F.; Wieghardt, K. *Inorg. Chem.* **2002**, *41*, 4179.

Table 3. Selected Bond Distances (Å)

			Complex **1**				
Ni−O1	2.038(1)	O1−C1	1.350(2)	C9−N10	1.484(2)	N10−C11	1.440(2)
Ni−N7	2.102(1)	C1−C6	1.406(2)	C11−C12	1.393(2)	C11−C16	1.400(2)
Ni−N10	2.137(1)	C1−C2	1.419(2)	C12−C13	1.386(2)	C13−C14	1.398(2)
C4−C5	1.385(2)	C2−C3	1.395(2)	C14−C15	1.395(2)	C15−C16	1.412(2)
C5−C6	1.395(2)	C3−C4	1.405(2)	O16−C16	1.370(2)	C8−C9	1.514(2)
C6−N7	1.461(2)	N7−C8	1.487(2)	O1···O16			
			Complex **2**[a]				
Ni−N47	2.012(2)	O1−C1	1.317(3)	N7−C8	1.298(3)	C8−C9	1.449(3)
Ni1−N7	2.014(2)	C1−C6	1.426(3)	C9−C10	1.286(3)	N10−C11	1.429(3)
Ni1−O1	2.056(2)	C1−C2	1.436(3)	C11−C12	1.387(3)	C11−C16	1.405(3)
Ni1−O41	2.084(2)	C2−C3	1.378(3)	C12−C13	1.401(3)	C13−C14	1.398(3)
Ni1−N10	2.166(2)	C3−C4	1.420(3)	C14−C15	1.402(3)	C15−C16	1.402(3)
Ni1−N50	2.193(2)	C4−C5	1.378(3)	O16−C16	1.368(3)		
C6−N7	1.383(3)	C5−C6	1.409(3)				
			Complex **3**				
Ni−N7	1.828(1)	Ni−O18	1.841(1)	N7−C8	1.458(2)	C10−N11	1.458(2)
Ni−N11	1.832(1)	Ni−O1	1.845(1)	N11−C12	1.360(2)	C12−C13	1.415(2)
O1−C1	1.312(2)	C1−C2	1.427(2)	C12−C17	1.436(2)	C13−C14	1.373(2)
C1−C6	1.434(2)	C2−C3	1.381(2)	C14−C15	1.429(2)	C15−C16	1.381(2)
C3−C4	1.427(2)	C4−C5	1.371(2)	C16−C17	1.429(2)	O18−C17	1.310(2)
C5−C6	1.417(2)	C6−N7	1.360(2)	C8−C9	1.528(2)	C9−C10	1.527(2)
			Complex **4**				
Pd(1)−N(7)	1.943(2)	Pd(2)−O(41)	1.9955(14)	C(10)−N(11)	1.448(3)	N(47)−C(48)	1.479(3)
Pd(1)−N(11)	1.944(2)	Pd(2)−O(57)	1.9963(14)	N(11)−C(12)	1.354(3)	C(48)−C(49)	1.524(3)
Pd(1)−O(17)	1.994(1)	Pd(2)−N(47)	2.0227(18)	C(12)−C(13)	1.419(3)	C(50)−N(51)	1.481(3)
Pd(1)−O(1)	1.997(1)	Pd(2)−N(51)	2.0250(17)	C(12)−C(17)	1.440(3)	N(51)−C(52)	1.465(3)
O(1)−C(1)	1.308(2)	Pd(2)−Pd(2)#1	3.0846(4)	C(13)−C(14)	1.365(3)	C(52)−C(53)	1.386(3)
C(1)−C(2)	1.431(3)	O(41)−C(41)	1.341(2)	C(14)−C(15)	1.427(3)	C(52)−C(57)	1.405(3)
C(1)−C(6)	1.440(3)	C(41)−C(46)	1.405(3)	C(15)−C(16)	1.380(3)	C(53)−C(54)	1.385(3)
C(2)−C(3)	1.380(3)	C(41)−C(42)	1.414(3)	C(16)−C(17)	1.426(3)	C(54)−C(55)	1.397(3)
C(3)−C(4)	1.427(3)	C(42)−C(43)	1.397(3)	O(17)−C(17)	1.310(2)	C(55)−C(56)	1.394(3)
C(4)−C(5)	1.366(3)	C(42)−C(59)	1.534(3)			C(56)−C(57)	1.415(3)
C(5)−C(6)	1.418(3)	C(43)−C(44)	1.398(3)			O(57)−C(57)	1.344(2)
C(6)−N(7)	1.353(3)	C(44)−C(45)	1.386(3)			C(49)−C(50)	1.523(3)
N(7)−C(8)	1.450(3)	C(44)−C(63)	1.531(3)			C(49)−C(67)	1.530(3)
C(8)−C(9)	1.535(3)	C(45)−C(46)	1.382(3)			C(49)−C(68)	1.549(3)
C(9)−C(10)	1.525(3)	C(46)−C(47)	1.473(3)				
			Complex **5**				
Cu(1)−O(20)	2.638(7)	C(3)−C(4)	1.415(12)	C(1)−C(6)	1.415(12)	N(7)−C(8)	1.288(11)
Cu(1)−O(1)	1.920(6)	C(4)−C(5)	1.359(13)	C(1)−C(2)	1.429(14)	C(8)−C(9)	1.484(12)
Cu(1)−N(7)	1.964(8)	C(5)−C(6)	1.395(14)	C(2)−C(3)	1.384(13)		
O(1)−C(1)	1.339(11)	C(6)−N(7)	1.417(13)				

[a] Data for only one crystallographically independent neutral molecule in crystals of **2**·5/8CH_2Cl_2 are given here.

The dangling *o*-aminophenol part exhibits the same geometrical features as those in **1** with the exception of the sp^2 phenyl−nitrogen bond which is slightly shorter in **2** at 1.43 ± 0.01 Å than the corresponding sp^3 phenyl−nitrogen bond in **1** at 1.46 ± 0.01 Å. It is clearly an aromatic *o*-aminophenol half which also forms an intramolecular O−H···O bond (O1···O56, 2.697(4); O16···O41, 2.764(4) Å).

The most significant difference between *O*,*N*,*N*-coordinated $(H_3L^1)^-$ in **1** and $(HL^2)^-$ in **2** is that the *O*,*N*-coordinated half of $(HL^2)^-$ in **2** is apparently not aromatic: the six C−C bond lengths are not equidistant. Significantly, they apparently exhibit the typical quinoidal distortions characteristic for an *o*-iminobenzosemiquinonate(1−) radical, $(L^{ISQ})^{-\bullet}$, as shown in Chart 1. Concomitantly, the bridging ethylenediimine part is also distorted in a characteristic fashion: the C−C bond is too short for a C−C single bond, and both C−N bonds are slightly too long for a typical >C═N− double bond. These bond lengths are more typical for an α,α-diimine radical anion.[12,21] Therefore, we propose that the singlet diradical resonance structure **B** in Scheme 2 plays an important role.

Figure 8 displays the structure of the neutral molecule [Ni($L^{3\bullet\bullet}$)] in crystals of **3**. The nickel(II) ions are in a square planar ligand environment where the two *o*-iminobenzosemiquinonate(1−) π radical anions are *cis* relative to each other due to the presence of the saturated, bridging 2,2-dimethylpropylenediamine moiety. The geometrical details of the *O*,*N*-coordinated radical anions are within experimental error identical to those reported for $[Ni^{II}(L^{ISQ})_2]$[2] and $[Pd^{II}(L^{ISQ})(bpy)]PF_6$.[7]

The crystal structure of **4** is interesting, since it reveals the presence of two different neutral molecules, namely, mononuclear $[Pd^{II}(L^{3\bullet\bullet})]$ (**4a**) shown in Figure 9 and $[Pd^{II}(H_2L^3)]_2$ (**4b**) shown in Figure 10, which is assembled as a dimer in the solid state via four N−H···O hydrogen bonds.

(21) Gardiner, M. G.; Hanson, G. R.; Henderson, M. J.; Lee, F. C.; Raston, C. L. *Inorg. Chem.* **1994**, *33*, 2456.

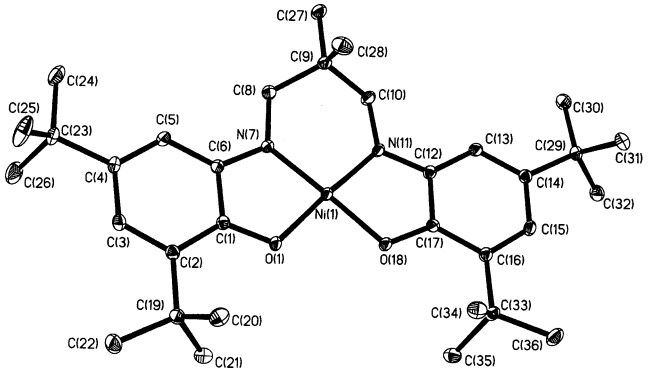

Figure 8. Structure of a neutral molecule $[Ni^{II}(L^{3\bullet\bullet})]$ in crystals of **3**.

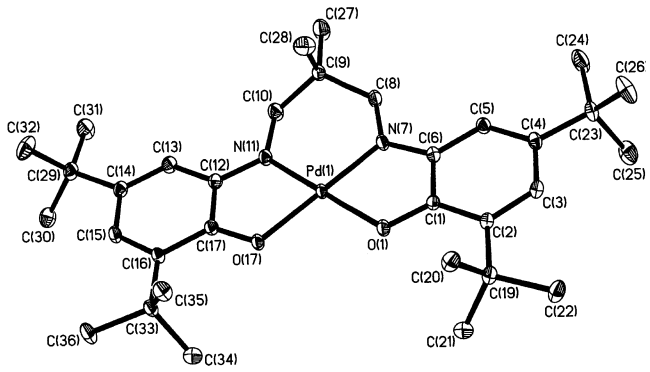

Figure 9. Structure of a neutral molecule $[Pd^{II}(L^{3\bullet\bullet})]$ (**4a**) in crystals of **4**.

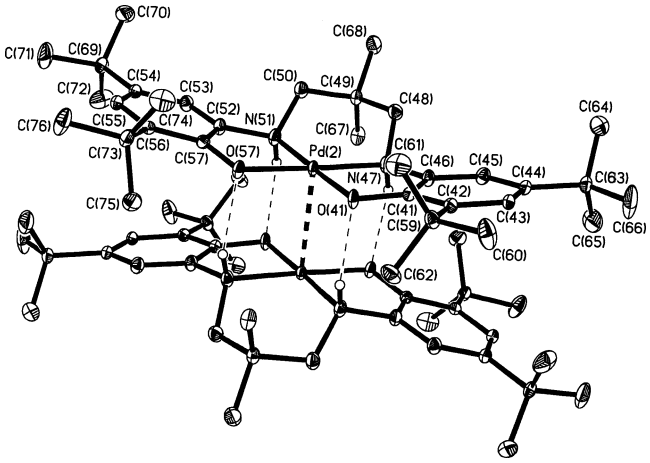

Figure 10. Structure of a neutral dimer $[Pd^{II}(H_2L^3)]_2$ (**4b**) in crystals of **4**.

Two N−H groups of half of a dimer form a contact to two phenolate oxygen atoms of the second half. The two halves of $[Pd(H_2L^3)]_2$ adopt an eclipsed configuration and give rise to an intramolecular Pd···Pd distance of 3.0846(4) Å which is a nonbonding contact, since the d_{z^2} orbitals of both Pd^{II} ions are filled. Note that similar metal−metal distances have been identified in refs 22 and 23 where weak direct metal−metal bonds prevail. The structure determination of **4** clearly shows the presence of two *O*,*N*-coordinated *o*-iminobenzosemiquinonate(1−) π radical anions in **4a** as in **3** and $[Pd^{II}(L^{ISQ})_2]$, but in the dimer **4b**, the two ligand halves are clearly aromatic and the two nitrogen atoms are sp^3 hybridized. The geometrical features are those of *O*,*N*-coordinated $(L^{AP})^-$ ligands (Chart 1) as in $[Mn^{III}(L^{AP})(L^{ISQ})_2]$.[5]

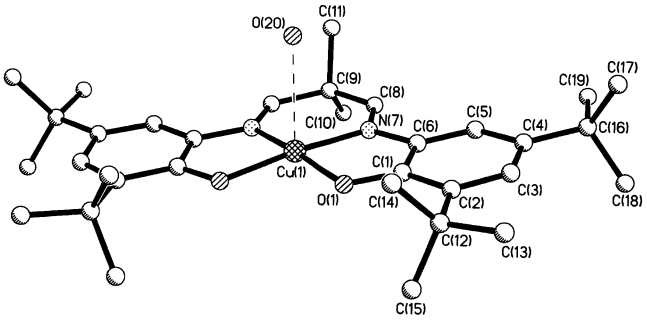

Figure 11. Structure of a neutral molecule $[Cu^{II}(OH_2)(L^4)]$ in crystals of **5**.

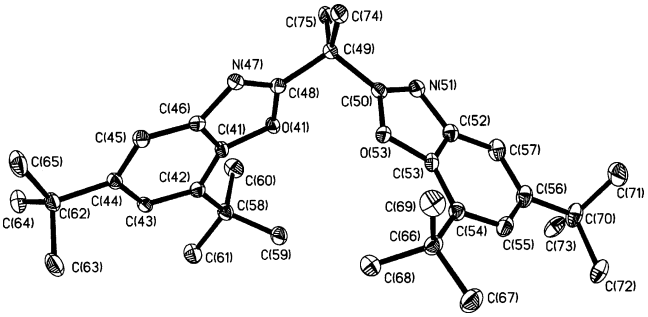

Figure 12. Structure of the oxidized ligand in crystals of **6**. Selected bond distances (Å): N47−C48, 1.283(3); C48−O41, 1.375(2); C41−O41, 1.384(2); C41−C46, 1.378(3); C46−N47, 1.405(3); C48−C49, 1.505(3).

The crystal structure of **5** shows that neutral molecules of $[Cu^{II}(OH_2)(L^4)]$ are present, as shown in Figure 11. Interestingly, the *O*,*N*-coordinated halves of the ligand $(L^4)^{2-}$ consist of aromatic iminophenolate(1−) moieties. Both nitrogen atoms are sp^2 hybridized and the C8−N7 distance at 1.29(1) Å is short and indicative of a carbon−nitrogen double bond. The crystal structure is of rather low quality with large estimated standard deviations. Therefore, we refrain from a more detailed discussion of the structure.

Finally, Figure 12 exhibits the crystal structure of the oxidized ligand **6**, which is a benzoxazol derivative.

EPR Spectra. The X-band EPR spectra of the electrochemically generated monoanions of **3** and **4** in frozen CH_2Cl_2 solutions at 10 K are shown in Figures 13 and 14, respectively. Both spectra display a rhombic $S = {}^1/_2$ signal with significant *g* anisotropy. Similar spectra have been reported for all square planar monoanionic complexes of the type $[M^{II}(L^{AP}-H)(L^{ISQ})]^-$, where $(L^{ISQ})^-$ is a benzosemiquinonate π radical and $(L^{AP}-H)^{2-}$ is its one-electron reduced aromatic form.[2,15−18] In contrast, the EPR spectrum of the monocation of **4a** with a $S = {}^1/_2$ ground state, namely $[Pd^{II}(L^{ISQ})(L^{IBQ})]^+$, where (L^{IBQ}) represents the one-electron-oxidized, neutral quinone form of half of $(L^{3\bullet\bullet})^{2-}$, is nearly isotropic and shown in Figure 14 (top). The g_{iso} value 2.0024 is in excellent agreement with the notion that the unpaired electron resides on the ligand in a π^* orbital. Very similar

(22) Herebian, D.; Bothe, E.; Neese, F.; Weyhermüller, T.; Wieghardt, K. *J. Am. Chem. Soc.* **2003**, *125*, 9116.
(23) (a) Millar, M.; Holm, R. H. *J. Am. Chem. Soc.* **1975**, *97*, 6052. (b) Reng, S.-M.; Ibers, J. A.; Millar, M.; Holm, R. H. *J. Am. Chem. Soc.* **1976**, *98*, 8037. (c) Peng, S.-M.; Goedken, V. L. *J. Am. Chem. Soc.* **1976**, *98*, 8500.

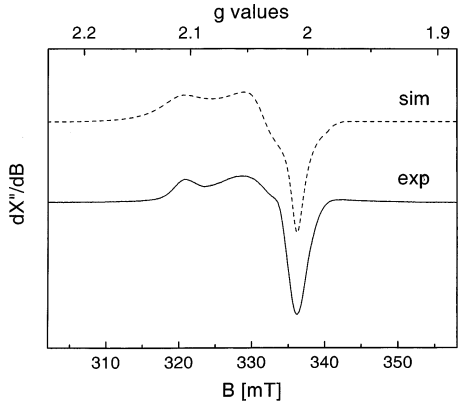

Figure 13. X-band EPR spectrum of the electrochemically generated monoanion of **3** in frozen CH_2Cl_2 solution (0.10 M $[N(n\text{-}Bu)_4]PF_6$) at 10 K. Conditions: 9.45257 GHz; modulation, 10 G; power, 0.2 nW. Simulation: $g_x = 2.0098$, $g_y = 2.0384$, $g_z = 2.1097$.

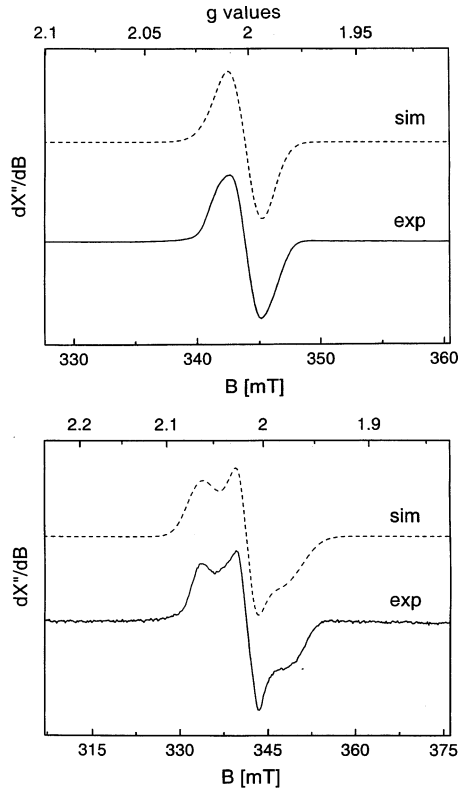

Figure 14. X-band EPR spectra of the electrochemically generated monocation (top) and of the corresponding monoanion (bottom) of **4a** in frozen CH_2Cl_2 solution at 10 K (0.10 M $[N(n\text{-}Bu)_4]PF_6$). Conditions: (top) frequency, 9.63497 GHz; modulation, 10 G; power, 0.2 nW; (bottom) frequency, 9.63564 GHz; modulation, 10 G; power, 0.2 nW. Simulation: (top) $g_x = 2.0007$, $g_y = 2.0007$, $g_z = 2.0058$, $g_{iso} = 2.0024$; (bottom) $g_x = 1.9763$, $g_y = 2.0154$, $g_z = 2.0645$.

spectra have been reported for $[M^{II}(L_O^{ISQ})(L_O^{IBQ})]^+$ and $[M^{II}(L_S^{ISQ})(L_S^{IBQ})]^+$ (M = Pd or Pt).[2,15−18]

In previous work,[7,24] we have shown from DFT calculations for $[M^{II}(L^{ISQ})_2]$ complexes that the two molecular orbitals shown in Figure 15 are highest in energy. These two MOs are basically the symmetric and antisymmetric combination of the singly occupied molecular orbital (SOMO) of the free semiquinonate ligand. In the neutral bis(semiquinonato)metal(II) species (**3** and **4a**), two electrons occupy the two close lying a_2 and b_2 orbitals. This situation gives rise to near-degeneracy effects and a pronounced diradical character of the neutral complexes. In the monocation, the b_2 orbital contains only a single unpaired electron. Due to symmetry reasons, the b_2 orbital cannot mix with any metal d orbital. Consequently, metal hyperfine coupling cannot be expected and is not observed experimentally. The lack of metal character in the b_2 SOMO makes the spin−orbit coupling of excited states with the ground state very inefficient, and therefore, the *g* shifts are expected to be very small in agreement with experiment.

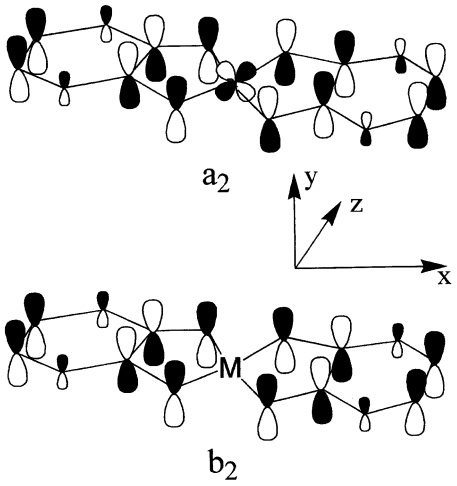

Figure 15. Highest two MOs in **3** and **4a**.

In contrast, in the monoanions of **3** and **4a**, the b_2 orbital is occupied by two electrons and the a_2 orbital is the delocalized SOMO. As shown in Figure 15, this orbital mixes with a d orbital of the metal ion which acquires thereby some metal character. This usually gives rise to sizable first-order hyperfine couplings. Since the ground state (A_2) readily mixes with relatively low lying d−d excited states, it also has a sizable orbital angular momentum which manifests itself experimentally in large *g* shifts. This is observed for the monoanions of **3** and **4a**.

Conclusions

The most salient features of the present study are summarized as follows:

(1) Complexes **1** and **2**, containing two tridentate saturated $(H_3L^1)^-$ and two unsaturated $(HL^2)^-$ ligands, respectively, both possess an $S = 1$ ground state, but their electronic spectra (Figure 1) differ significantly. From low-temperature X-ray crystallography of **1** and **2**, it is clearly established that only in **1** the *O*,*N*-coordinated *o*-iminophenolate part of $(H_3L^1)^-$ is aromatic with six equivalent C—C bonds in each ring. In contrast, the equivalent bond distances of the *O*,*N*-coordinated part of the unsaturated ligand $(HL^2)^-$ in **2** displays quinoid-type distortions characteristic of *O*,*N*-coordinated *o*-iminobenzosemiquinonate(1−) π radicals and, concomitantly, the bridging ethylenediimine part also shows a too short C—C single bond and two too long C═N double bonds. Thus, it is obvious that the singlet diradical resonance structure **B** in Scheme 2 contributes significantly to **2**. This

(24) Herebian, D.; Wieghardt, K.; Neese, F. *J. Am. Chem. Soc.* **2003**, *125*, 10997.

is supported by intense ligand-to-ligand charge transfer bands in the visible spectrum of **2**.

(2) The properties of **3** and **4a** are typical for square planar, singlet diradicals[2] including the observation of a complete electron transfer series for each species. The EPR spectra of their corresponding monocations and monoanions have been interpreted in terms of two differing ligand centered SOMOs of which the b_2 SOMO lacks metal character, whereas the a_2 ligand orbital mixes significantly with metal d orbitals. This is the origin of the differing *g* anisotropy of the EPR spectra of the monoanions and -cations, both of which possess $S = {}^1/_2$ ground states.

(3) Finally, air oxidation of $H_4[L^3]$ in the presence of Cu^{II} ions does not yield $[Cu(L^{3\bullet\bullet})]$ but instead yields $[Cu^{II}(H_2O)(L^4)]$, containing two aromatic iminophenolate moieties (oxidative Schiff base formation).

Acknowledgment. This work was supported by the Fonds der Chemischen Industrie. K.S.M. is grateful to the Max-Planck Society for a postdoctoral fellowship.

Supporting Information Available: Crystallographic data files for complexes **1**, **2**, **3**, **4**, **5**, and **6**. This material is available free of charge via the Internet at http://pubs.acs.org.

IC0302480